Effects of atmospheric particle concentration on cloud microphysics over Arecibo

Daniel E. Comarazamy,[1] Jorge E. Gonzalez,[2] Craig A. Tepley,[3] Shikha Raizada,[3] and R. V. R. Pandya[1]

Received 19 May 2005; revised 1 November 2005; accepted 8 February 2006; published 13 May 2006.

[1] A new cloud microphysics module incorporated to a regional atmospheric model and atmospheric particle (AP) observations performed at the Arecibo Observatory were used to simulate two short precipitation events observed in the area of the observatory and to investigate the possible effects of AP on cloud formation and rain development. First, model runs were performed with and without the new cloud module, initialized with the new AP data set and the previous cloud spectrum available. The combination of the new cloud module and the Arecibo observations produced the most satisfactory results and significant improvements in total precipitation modeled: 70 versus 80 mm observed. The improvement results in 15% more precipitation predicted when compared with the old cloud information and more than 50% with respect to simulations without cloud condensation nuclei activation. Then, a set of idealized runs showed that cloud droplet production is significantly larger in polluted air than in clear skies and that rainwater in polluted air is less than that in unpolluted air. This may be because existing droplets will compete more vigorously for the available water vapor and will not reach the necessary radius to fall, and therefore growth by collision and coalescence is subdued.

Citation: Comarazamy, D. E., J. E. Gonzalez, C. A. Tepley, S. Raizada, and R. V. R. Pandya (2006), Effects of atmospheric particle concentration on cloud microphysics over Arecibo, *J. Geophys. Res.*, *111*, D09205, doi:10.1029/2005JD006243.

1. Introduction

[2] The interaction between clouds and aerosols is being recognized as one of the major factors controlling cloud development and precipitation patterns over local, regional, and even global scales. Given the complexity of the problem due to the intricate physics of cloud formation and development, in-cloud turbulence, aerosol chemistry and dynamics, among other topics, progress in this area has been hindered, or oversimplified for a long time. During recent years there have been significant advances in cloud microphysics, cloud modeling schemes, cloud-resolving atmospheric models, and in computing capabilities that could improve our ability to predict the effects of atmospheric particles (AP) on different cloud microphysical fields over tropical regions.

[3] The main mechanism where AP influences the development of clouds and precipitation, is when new particles serving as condensation nuclei increase the number of small droplets. The spectrum of these new drops depends on the characteristic of the AP. The higher concentration damps the growth of existing cloud droplets by diffusion because there will be more competition for the water vapor available in the atmosphere. This, in turn, affects the possibility of growth by collision and coalescence because the effective drop radius for this process to occur cannot be reached. *Khain et al.* [2000] reported several studies in polluted areas over Thailand and Indonesia where observed smoky clouds do not precipitate altogether, having narrow spectra of small droplets. At the same time, similar clouds precipitate in unpolluted air in only 15–20 min after their formation. Similar results were found in continental clouds of Amazon smoky areas [*Kaufman and Nakajima*, 1993].

[4] Highly idealized simulations of the tropical climate using a cloud-resolving model showed that cloud microphysics appears to have minor effects on the large-scale flow as well as on temperature and moisture profiles [*Grabowski et al.*, 1999; *Grabowski*, 2000, 2003]. Changes in cloud microphysical parameters in these experiments have a dramatic impact on the quasi-equilibrium ocean temperature. Large cloud and raindrops produced sea surface temperatures (SSTs) between 37° and 38°C, and in the range of 32°–35°C in the simulation with small particles. The approach used by the authors followed the development of convection in response to large-scale flow at timescales much larger than the life cycle of observed clouds. The effects of cloud microphysics on surface processes are paramount by modifying surface sensible and latent heat fluxes. One key note made by *Grabowski et al.* [1999] is that smaller cloud drops, and a slower conversion of cloud

[1] Mechanical Engineering Department, University of Puerto Rico, Mayagüez, Puerto Rico.
[2] Mechanical Engineering Department, Santa Clara University, Santa Clara, California, USA.
[3] National Astronomy and Ionosphere Center, Arecibo Observatory, Arecibo, Puerto Rico.

0148-0227/06/2005JD006243

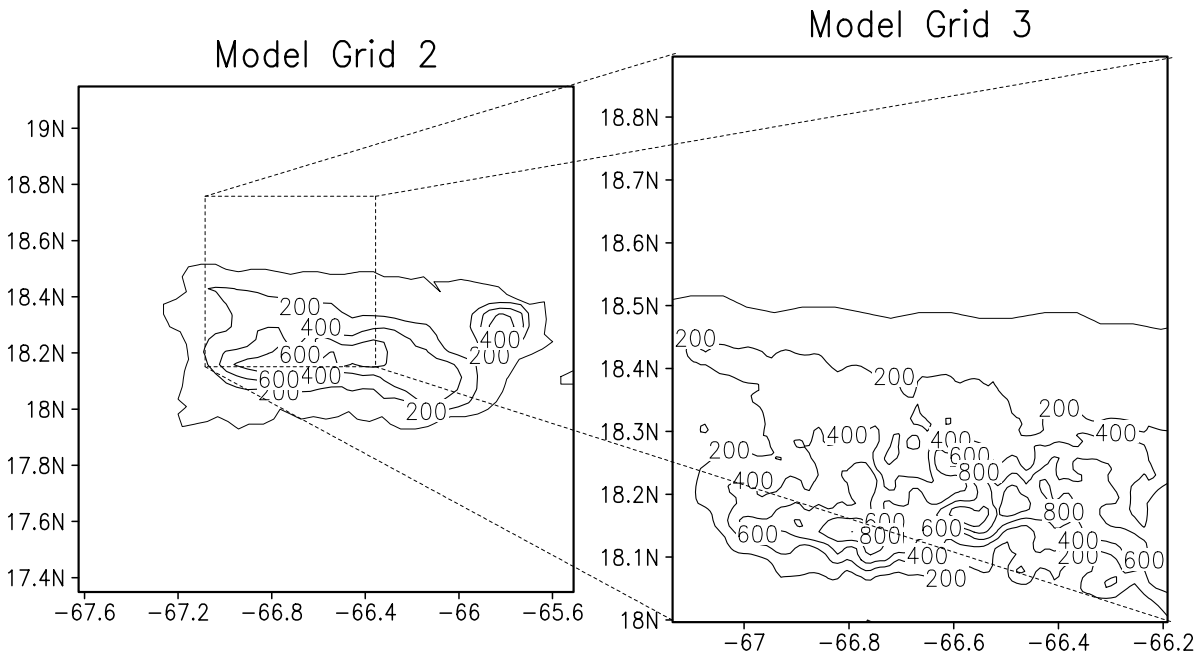

Figure 1. Topography of the Island of Puerto Rico (contour interval 200 m) and area centered on the Arecibo Observatory where the study was performed (expanded inset, contour interval 200 m).

water to rain, results in enhanced cloud mass fluxes, a colder and drier boundary layer, larger surface fluxes, a warmer and more humid free atmosphere, and a lower convective available potential energy.

[5] Of interest to the Caribbean region are the findings of *Wang* [2002], who using the tropical cyclone model, showed that the cloud structure of the simulated storm can be quite sensitive to the details of the cloud microphysics parameterization. However, the intensification rate and final intensity do not vary too much. This indicates the potential advantage in using explicit cloud microphysics in tropical cyclone simulations to improve the intensity forecasting. Similar results are found using mesoscale atmospheric models with the inclusion of microphysics parameterization schemes [*Liu et al.*, 1997]. *Li et al.* [2002] used a 2-D cloud-resolving model to explain and study the dominant cloud microphysical processes associated with a tropical oceanic convective system. *Jonas* [1996] theorized about the effects of in-cloud turbulence on the growth of cloud droplets by condensation and coalescence in low-level water clouds, but such an analysis is beyond the scope of the work presented here.

[6] The intention of this paper is to demonstrate an improvement in our ability to predict precipitation in tropical coastal regions by using a better representation of cloud microphysics and a local AP spectrum. With the aide of a cloud resolving mesoscale model and detailed AP observations by the Arecibo Observatory (AO) we present in this work the ability of a mesoscale model to simulate a precipitation event identified in the region of interest. A second set of model runs will try to explain the dissimilarity in resolved total precipitation between the different predictions of the same precipitation event. The area of study is located on the north coast of the Caribbean island of Puerto Rico, centered on the Arecibo Observatory (18.35°N, 66.75°W), as shown in the model grids used (Figure 1).

2. Atmospheric Particle Measurements

[7] The aerosol measurements generally were made from two locations in northwest Puerto Rico (at the Arecibo Observatory and near the town of Aguadilla (18.50°N, 67.13°W)) that represent rural inland and suburban coastal conditions, respectively. The instrument used is a five-channel portable Sun photometer called the Microtops II manufactured by Solar Light, Inc [*Ichoku et al.*, 2002]. The channels are filtered for 380, 440, 500, 675, and 870 nm, but these wavelengths are supplemented with additional radiance measurements at 305, 312, and 320 nm in the near UV (used to determine columnar ozone), and with 936 and 1020 nm in the near IR (used to determine water vapor), using a different instrument from Solar Light. Although ozone and water vapor measurements are important input to climate models, in this paper only the aerosol optical thickness data determined from six, sometimes seven, of the wavelengths observed with these two instruments were used. These span the optical spectrum from the near UV to the near IR, which allows us to extract particle sizes to almost three orders of magnitude. Calibration is important, and the filter transmission and detector sensitivity of these instruments are cross-checked against other optical standards, such as Dobson spectrophotometers, on a yearly basis.

[8] From as early as March 2002, measurements of transmitted atmospheric radiance, and thus the aerosol optical thickness (AOT) at the wavelengths mentioned above have been taken, with an average of two and three observations per day (usually at 0900, 1200, and 1500 LT where solar zenith angles are less than about 45°). These AOT data can be inverted to estimate the size of the

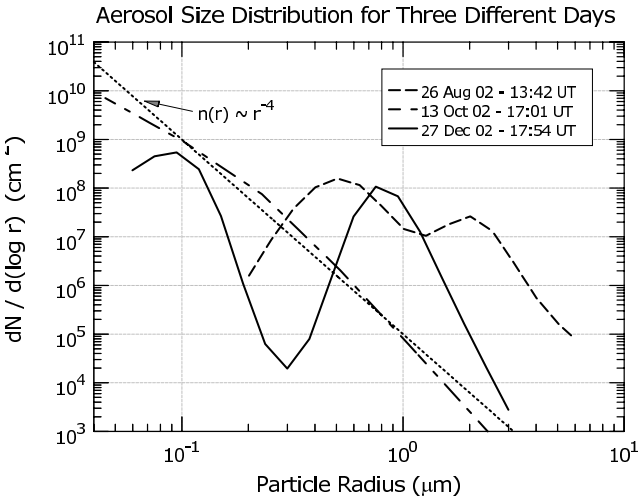

Figure 2. Log-radius number distribution for aerosols as a function of particle radius measured from northwest Puerto Rico on 3 days. Illustrated are three different and distinct distributions that are most characteristic of water soluble (December), a dusty environment (August), and a general Junge distribution (October) where aerosol number density decreases with increasing particle radius, r, at a rate of r^{-4}.

particles that are responsible for the extinction of solar radiation, and this provides better estimates for the cloud condensation nuclei to be used in the climate models. The code developed by *King et al.* [1978] and *Dubovik and King* [2000] was used for the inversions. The range of the inversion spans the smaller, Aitken-type particles ($r < 0.1$ μm) through the Large ($0.1 \leq r \leq 1.0$ μm) and Giant ($r > 1.0$ μm) aerosol classifications for particle radius, r. The lower limit of the inversion technique obtained overlaps with what might be considered true cloud condensation nuclei (CCN) and as such, provides a good estimate of the seasonal behavior of CCN in the tropics. An example of estimated aerosol particle size distribution for three separate days in 2002 is shown in Figure 2.

[9] Figure 3 shows the annual variation of the number density for several particle radii extracted from the inversion algorithm. The range is logarithmic and skewed toward the smaller radii. There are a few interesting features of the data presented in Figure 3 of aerosol size variation. For example, seasonal variations exist in the aerosol optical thickness (AOT) data that we observe in Puerto Rico. We have found that AOT at shorter (blue) wavelengths tends to maximize near the equinoxes (together with minima during the solstices), while variations at longer wavelength AOT maximize in the summer months, nearly two orders of magnitude more when compared with the winter months. That is, a general "out-of-phase" condition exists between longer and shorter wavelengths throughout the year, mirroring near the center of the observable spectra, or roughly near 0.5 μm. During the summer in the Caribbean, we often experience so-called "hazy" conditions in the atmosphere resulting from the transport of dust from the African Sahara desert across the Atlantic. The inversion of AOT to determine particle size reflects this trend, with the larger, dust-like particles appearing in the summer months with a relative minimum amount of particles of smaller radii. The relative increased presence of smaller particles during the equinoxes, along with their reduction in the summer compared with the larger particles, is consistent with the timing of the Caribbean two rainy seasons, as well as with a reduction of rainfall during the summer, when the midsummer drought occurs [see *Daly et al.*, 2003; *Malmgren and Winter*, 1999; *Taylor et al.*, 2002].

3. Model Description

[10] The mesoscale model used in this work is the Regional Atmospheric Modeling System (RAMS), developed at Colorado State University [*Pielke et al.*, 1992; *Walko et al.*, 1995a, 1995b; *Cotton et al.*, 2003]. RAMS is a highly versatile numerical code developed for simulating and forecasting meteorological phenomena. The atmospheric model is built around the full set of nonhydrostatic, dynamical equations that governs atmospheric dynamics and thermodynamics, plus conservation equations for scalar quantities such as mass and moisture. These equations are complemented by a large selection of parameterizations available in the model.

[11] The RAMS version used in this research contains a new cloud microphysics module described by *Saleeby and Cotton* [2004], a development from the current microphysics package [*Meyers et al.*, 1997; *Walko et al.*, 1995c]. The two major differences of this new RAMS cloud microphysics module are the activation of cloud condensation nuclei (CCN) and giant CCN (GCCN) through the use of a Lagrangian parcel model that considers ambient cloud conditions for the nucleation of cloud droplets from aerosol, and a new cloud water hydrometeor category. The large-droplet mode was included to represent the dual modes of cloud droplets that often appear in nature [*Berry and Reinhardt*, 1974; *Nagel et al.*, 1998]. This inclusion serves as a middle step in the growth of cloud droplets. Currently, cloud drops do not grow from 2 to 40 μm in diameter, and

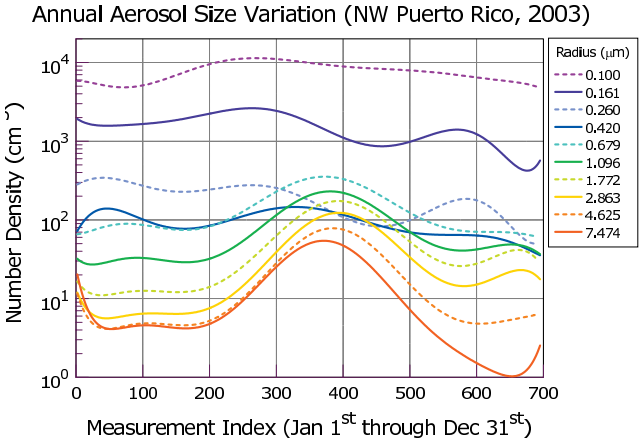

Figure 3. Annual variation of the number density as a function of aerosol particle size measured in Puerto Rico. The data resulted from the inversion of radiometric observations of aerosol optical thickness that were made at several discrete wavelengths from the near UV to the near IR of the optical spectrum.

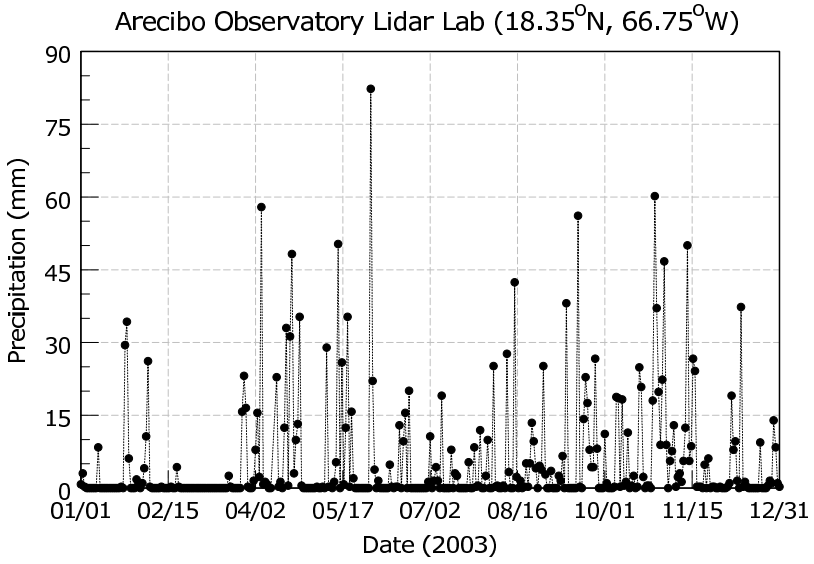

Figure 4. Arecibo Observatory Station daily precipitation totals for 2003.

then jump to the next hydrometeor category (rain) that is considerably larger, but instead there is another cloud droplet (from 40 to 80 μm in diameter) category that allows a slower drop growth. Therefore, for liquid phase hydrometeors, the following collisions are possible: cloud1-cloud1, cloud1-cloud2, cloud2-cloud2, cloud1-rain, cloud2-rain, and rain-rain, where cloud1 and cloud2 represent the small and large cloud droplet modes respectively, and rain the raindrops.

[12] RAMS employs lookup tables of autoconversion rates generated from bin model computations based on the assumed bulk distribution functions. CCN and GCCN are allowed to deplete upon activation and to replenish upon liquid hydrometeor evaporation. Another inclusion is that RAMS now has the option for one- and two-moment prediction for both cloud categories. If both cloud categories are predicted with two moments, and CCN/GCCN are activated, the user may specify the nuclei concentration (cm^{-3}) and the distribution median radius (r_g), possible specifications of these parameters now include a domain-wide homogeneous field (used in this research), a horizontally homogeneous vertical profile, and a 3-D variable field. The user also specifies the shape parameter of the hydrometeor gamma distributions. From this information, the

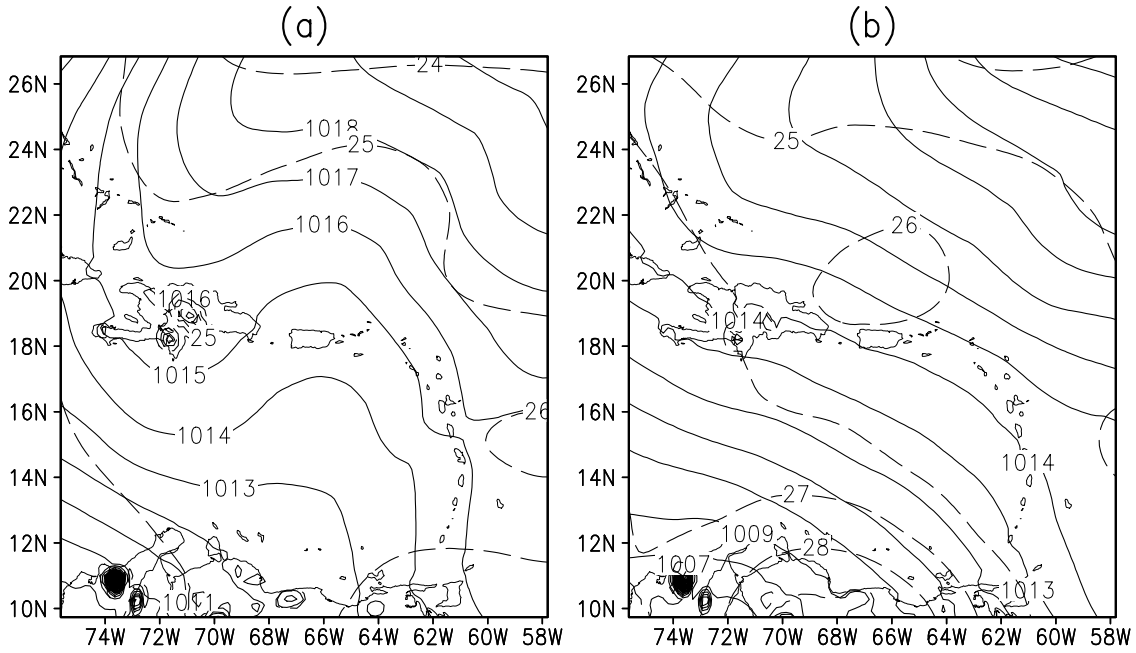

Figure 5. Synoptic surface analysis of sea level pressure (solid lines) and temperature (dashed lines), contoured every 1 mbar and 1°C respectively, for (a) 0800 LST 2 June 2003 and (b) 2000 LST 2 June 2003.

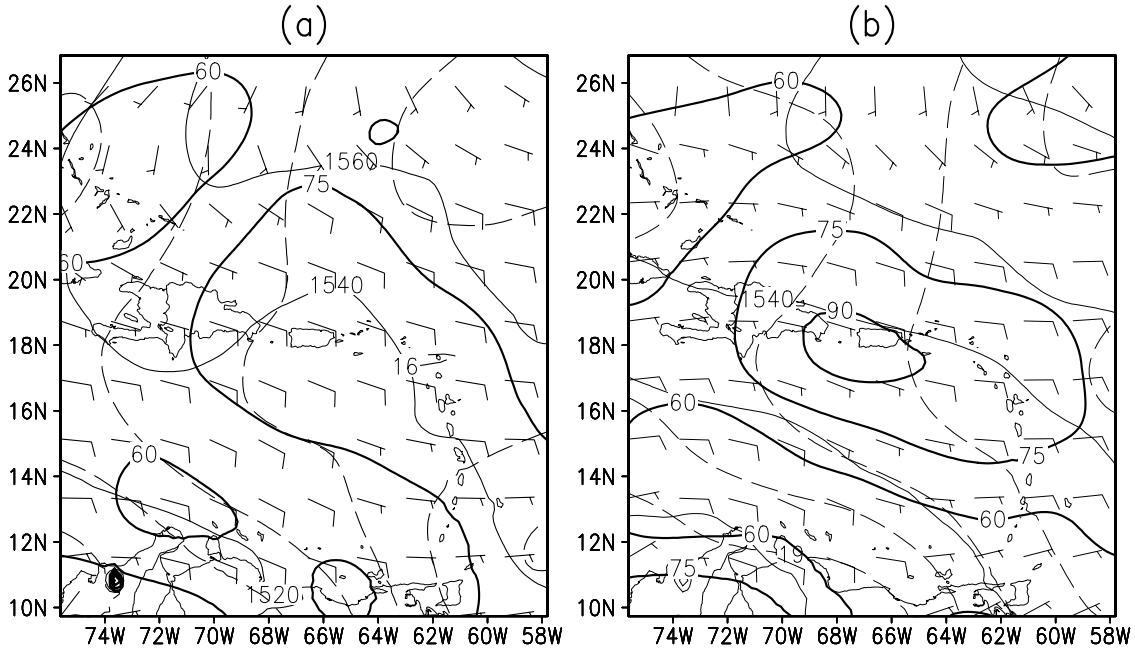

Figure 6. Synoptic upper air 850 mbar analysis of geopotential height (thin solid line) contoured every 20 m, temperature (dashed line) every 1°C, and relative humidity (thick solid line) in 15% intervals for (a) 0800 LST 2 June 2003 and (b) 2000 LST 2 June 2003.

CCN/GCCN masses are calculated from lookup tables. These lookup tables are essentially lognormal distributions of CCN/GCCN. Each table delineates between CCN and GCCN and contains 200 mass bins (from 10^{-19} to 10^{-8} g for CCN, and from 10^{-14} to 10^{-5} g for GCCN) and 14 possible median radii (from 0.01 to 0.96 μm for CCN, and from 1.5 to 5.5 μm for GCCN). Each distribution initially divides up the mass of only one CCN or GCCN (cm^{-3}) of a given size. Thus, to obtain the true distribution at a grid point, each bin of a set distribution for one CCN is multiplied by the true number of nuclei that are activated at a given time. The total mass, corresponding to the number of CCN, is determined by summing the mass in each bin of the distribution until this number is reached. For more information and details on the Lagrangian parcel model and the activation process, the reader is referred to *Saleeby and Cotton* [2004].

4. Simulating a Precipitation Event

[13] Maximum rainfall during 2003 was recorded on 2 June 2003 by the AO Weather Station, as shown in Figure 4. The precipitation recorded by the station was exactly 80.85mm of rain for that day. During the early hours of the day a sea level low-pressure gradient moved over the island of Puerto Rico while a relatively high-pressure region developed over Hispaniola, also observed in the surface synoptic map was a weak temperature gradient of the order of 3°–4°C. By late in the evening, the pressure gradient had disappeared while a hot spot remained just north of Puerto Rico (Figure 5). The 850mbar maps show an interesting situation of strong moisture and temperature advection into the Greater Antilles region of the Caribbean, which might have supplied the moisture required for the precipitation observed for that day, together with the lifting mechanism of the low-pressure region (Figure 6). At this level, the surface low pressure is still an identifiable feature as evidenced by a disturbance in the height field. Since all the experiments consists of short runs, nudged by the NCEP fields every 12 hours, no major changes in the simulated synoptic fields were expected. Hence the results presented and discussed will focus on total precipitation produced by the runs on the cloud microphysics resolving grid, namely grid 3.

4.1. Experimental and Model Configuration

[14] The first set of model experiments is several runs constructed around the new set of observations by the AO for the year of 2003 (see Figure 3). These were initialized using the AO data set, and NCEP atmospheric data to drive the model. A large, coarse grid of 20km is included in the configuration, not shown in Figure 1 and named grid 1, to perform the downscaling of the large-scale 2.5° × 2.5° NCEP data. A period of 7 days, centered on 2 June was first selected to attempt the replication of the precipitation event. The AP concentration information is updated accordingly to the frequency recorded by the AO. A second run was configured for 6 April of 2003 to validate the improvement in the predictions of precipitation.

[15] Besides being the day of maximum precipitation recorded by the Arecibo Observatory Station, 2 June 2003 is surrounded by calm days (especially with the absence of

Table 1. Ensemble Matrix of Runs for Experiment 1

	Microphysics Information	
Model Version	Arecibo Observations	Hawaii Cloud Spectrum
RAMS w/CCN/GCCN activation	run 1	run 2
RAMS 4.3	na	run 3

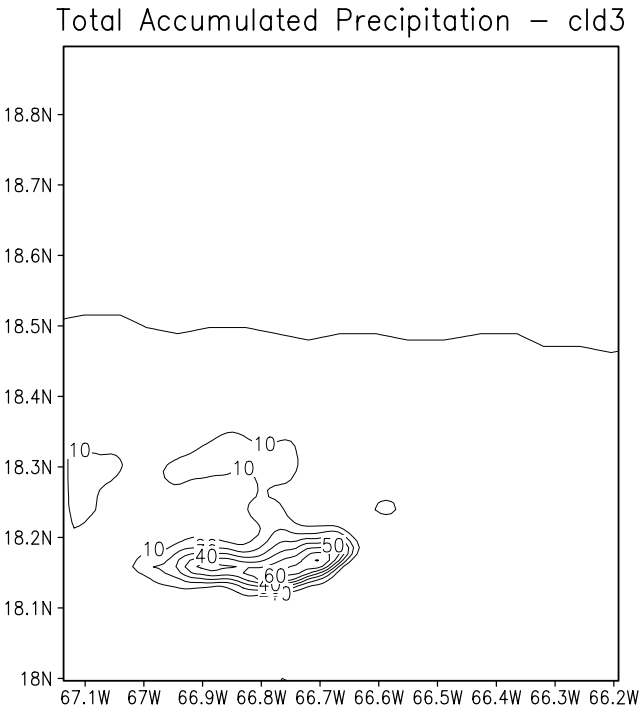

Figure 7. Spatial distribution of the total accumulated precipitation on grid 3 for the 7 day period of the numerical model simulation run 1.

rainfall), which is beneficial to the numerical simulation. By selecting an isolated precipitation event, the atmospheric model is allowed a period of time for stabilization, determined to be at three days given the actual grid configuration shown in Figure 1. The methodology of ingesting the AP information is to drive the model with an initial profile, then restarting the model after updating the AP profile at the times available in the data set provided by the AO team.

[16] In order to better separate the different influences on the results of the two model versions used, the atmospheric particle observations from the Arecibo Observatory, and the microphysical information previously available for this type of study and used in past modeling efforts (not described in this note), an ensemble of runs is suggested and is shown in Table 1. The cloud spectrum previously used was obtained with measurements of maritime cumulus clouds in Hawaii [*Rogers and Yau*, 1996]. The suggested simulations were performed with the same grid configuration and large-scale forcing, following the ensemble matrix.

4.2. Results

[17] After performing the simulations in the methodology explained above, the results for total accumulated precipitation were plotted and compared with the observations from the weather station. The maximum recorded precipitation by the station was about 80 mm of rain on the date 2 June 2003; the model simulated a total rainfall of approximately 70, 55, and 35 mm in the area of study for run 1, run 2, and run 3, respectively. Figure 7 shows the spatial distribution of total accumulated precipitation during the entire simulation run 1 for grid 3, run 2 followed the same spatial pattern but with smaller values. The spatial distribution of precipitation for run 3 differed significantly from run 1 and run 2.

[18] A time series of the precipitation predicted by the RAMS model shows that this precipitation was accumulated exactly during a 5 hour period in the early hours of 2 June. Figure 8 presents such a time series of total simulated precipitation for the location of maximum precipitation for run 1, run 2, and run 3. The new methodology and AP data set not only produces more liquid precipitation, but also is far

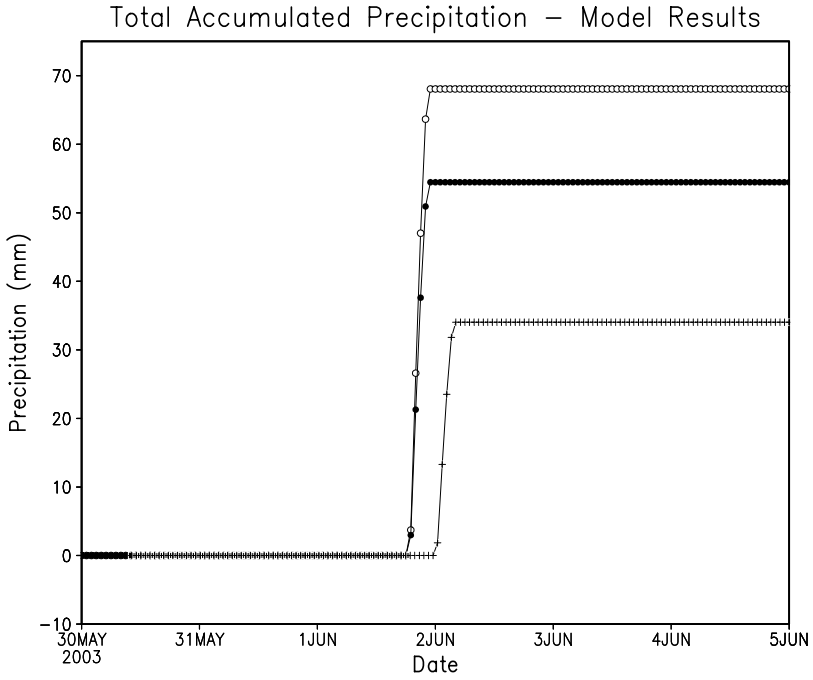

Figure 8. Time series of simulated maximum total precipitation for the simulations run 1 (open circles), run 2 (solid circles), and run 3 (crosses).

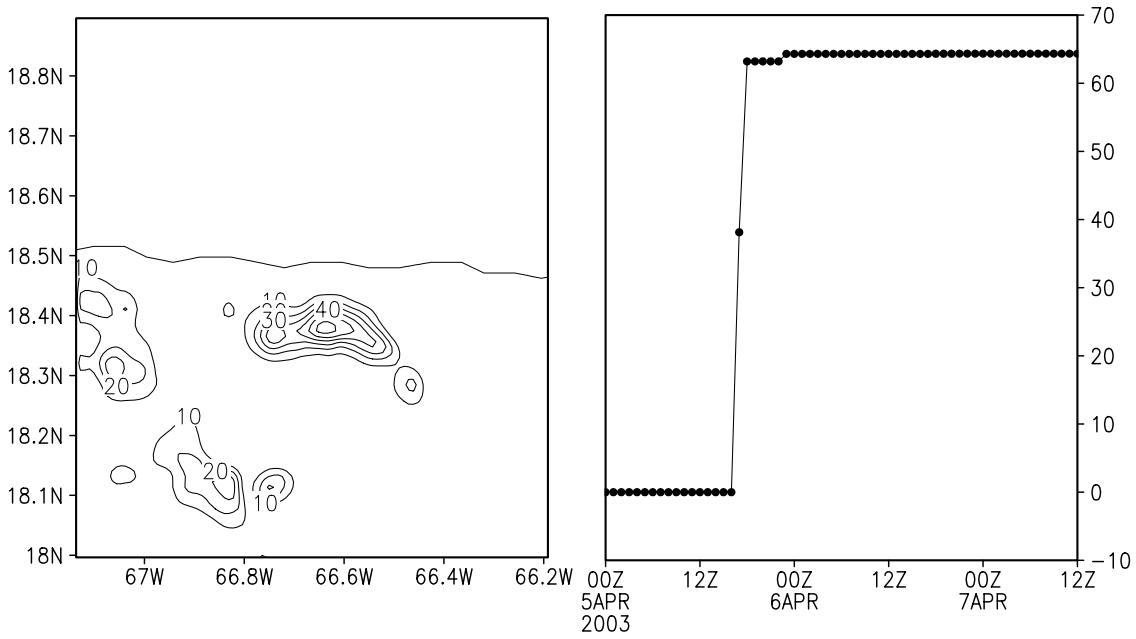

Figure 9. Spatial distribution of the total accumulated precipitation on grid 3 for run 4 (6 April 2003) and time series of simulated maximum total precipitation for the simulation.

more accurate in the prediction when comparing the results with observations. The higher amounts of precipitation and liquid water concentration are because the new AP information contains relatively lower concentrations during the day hours when convection typically occurs in the Puerto Rican coastlines. As will be discussed in the next section with the idealized experiments, unpolluted skies produce more rainwater in the atmosphere. This simple, but very real and detailed, experiment shows that the new microphysical module with CCN/GCCN activation is capable of satisfactorily replicating a single precipitation event when used with the AP data provided by the Arecibo Observatory.

[19] To demonstrate that the model is indeed capable of reproducing large amounts of precipitation observed over short periods of time with the new microphysics module and the Observatory AP observations, another simulation was set up following the same configuration of run 1. The day chosen was 6 April 2003, the second rainiest day of the year in the area of the Arecibo Observatory (Figure 4) with 68 mm of rainfall observed. The simulation is identified as run 4 and the results for total precipitation accumulated are shown in Figure 9. Here we can see that the model simulated an amount of precipitation almost identical to that recorded by the station, differing only by a few mm of rain, 63 mm modeled, demonstrating the model's ability to simulate these shorts events. It should be pointed out that the regional model used for this research has been proven to be more accurate in simulating monthly precipitation totals in Puerto Rico during the early rainy season, than during the late season in October, and there has not yet been an attempt to simulate a month in the midsummer drought [*Comarazamy*, 2001].

5. Semi-idealized Runs

[20] In order to have a better understanding of the difference in total resolved liquid precipitation between the simulations using the new cloud microphysics module driven with different microphysical information, a second set of experiments were designed to investigate the possible effects of pristine and polluted air on cloud formation and rain development over a limited geographical area.

5.1. Methodology and Experimental Setup

[21] The model runs are constructed and initialized from observations performed by the AO on 26 August 2002 and 27 December 2002 using aerosol data collected using radiometers. The atmospheric homogeneous AP profile for this data is shown in Figure 2. Here it is clearly seen the bimodal nature of AP in the region of study. In the future, we plan to use the lidar facilities at AO to observe vertical profiles of aerosols in the Puerto Rican atmosphere.

[22] The two sets of experiments will be referred to from here on as cld.1 (26 August 2002) and cld.2 (27 December 2002). The model runs are designed to simulate conditions of unpolluted and polluted skies from the data shown in Figure 2, which by itself represents the control run. Figure 2 includes data for 13 October 2002 that was not used in the numerical simulations. The experiments were performed with decreased AP concentration and increased concentrations, for the unpolluted and polluted runs respectively (low

Table 2. Ensemble Matrix of Runs and Parameters Used for Experiment 2[a]

		cld.1 dN/d(log r/R*) (cm^{-3})-r (μm)	cld.2 dN/d(log r/R*) (cm^{-3})-r (μm)
Low	CCN	$10^7-0.5$	$10^8-0.1$
Low	GCCN	10^6-2	10^7-1
Control	CCN	$10^8-0.5$	$10^9-0.1$
Control	GCCN	10^7-2	10^8-1
High	CCN	$10^9-0.5$	$10^{10}-0.1$
High	GCCN	10^8-2	10^9-1

[a]Where R* = 1 cm is a characteristic radius.

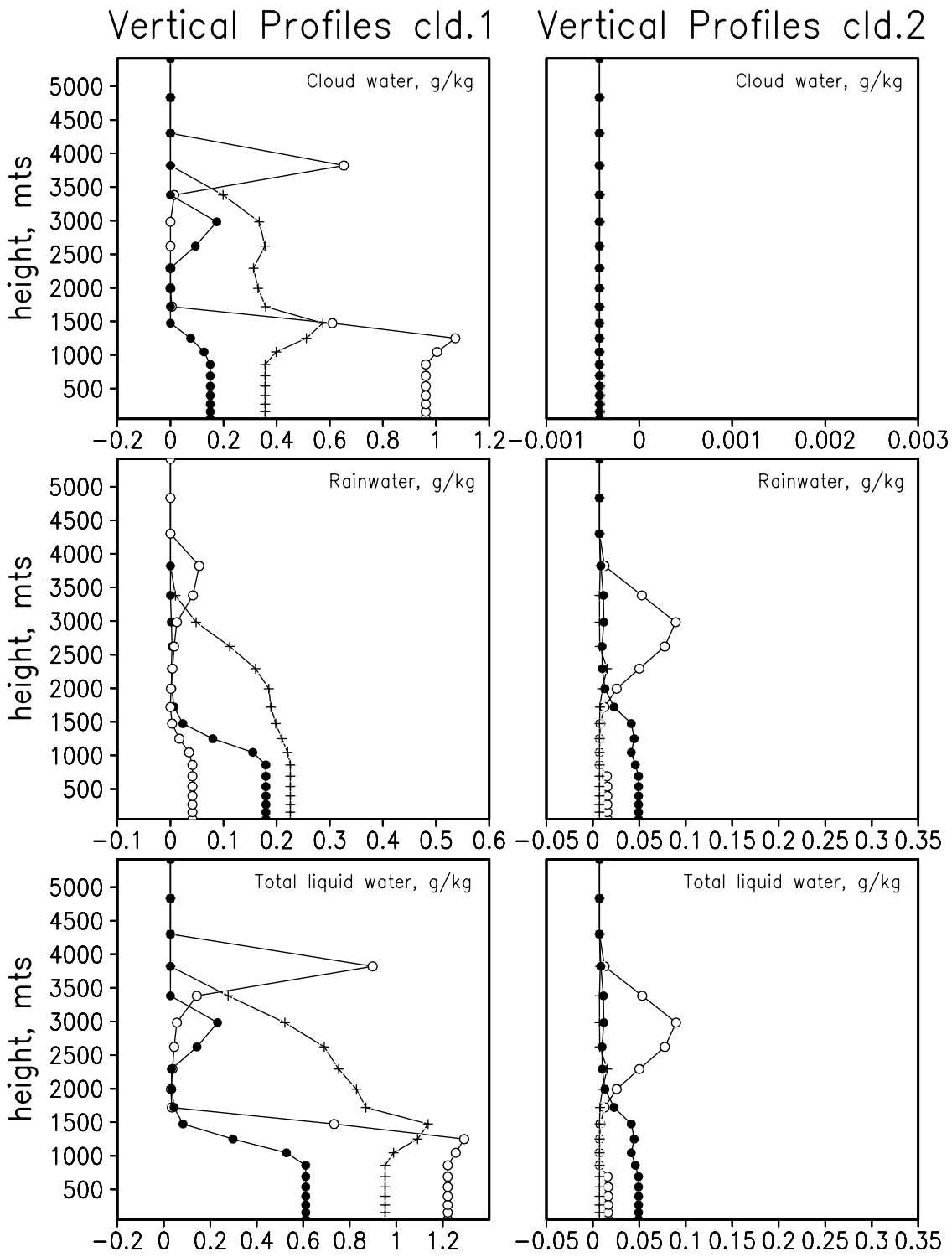

Figure 10. Vertical profiles of (top) cloud water, (middle) rainwater, and (bottom) total liquid water at the location and time of maximum convection for all experiments. Crosses, control; open circles, high; solid circles, low.

and high). The runs performed for experiment 2 are identified and summarized in Table 2.

[23] The semi-idealized, horizontally homogeneous runs were initialized using sounding data from each of the days when the AP measurements were taken, at the closest time available. The temperature of the lower atmospheric levels was increased by 5 K to stimulate convection, and therefore cloud formation and rainwater development. The different experiments were compared with the control run to study the effect of each one on these parameters. The microphysics moisture complexity was set to the highest level in RAMS. This level incorporates all categories of water in the

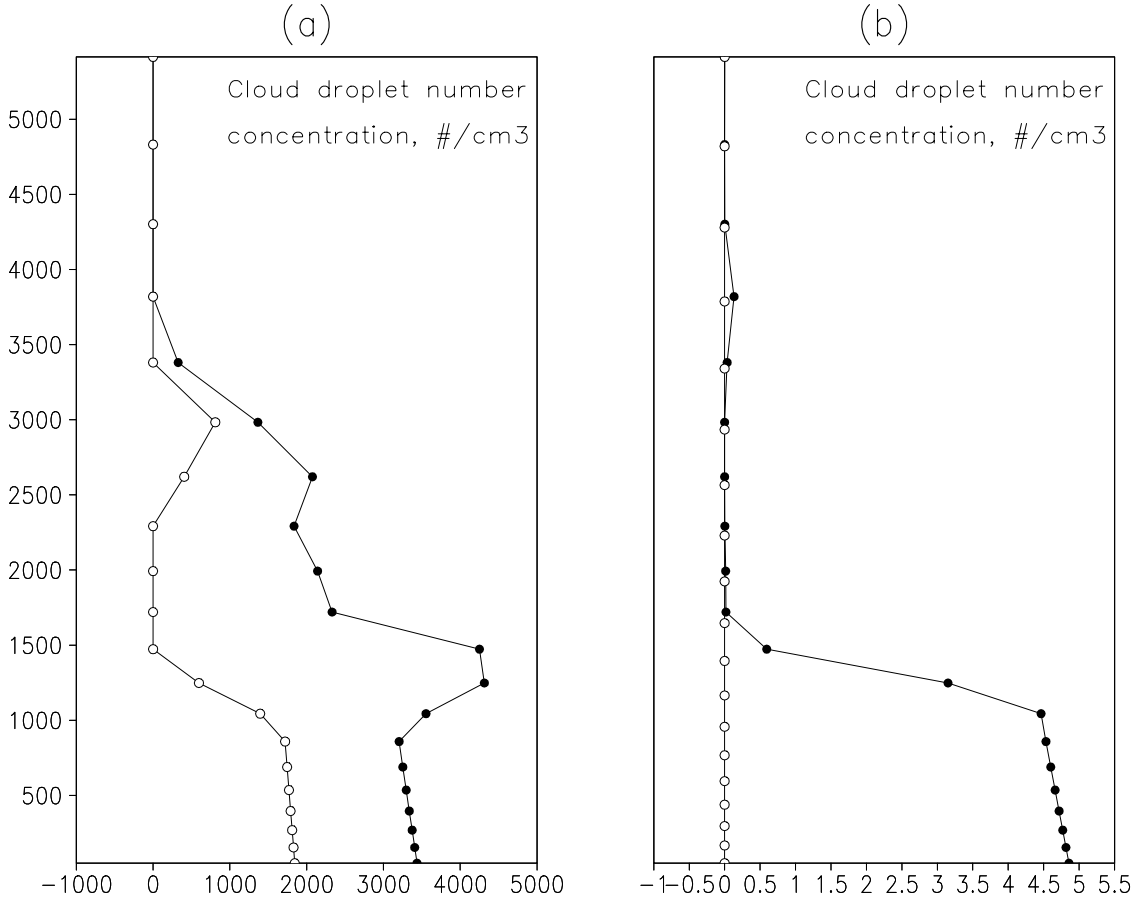

Figure 11. Vertical profiles of cloud droplet number concentration at the location and time of maximum convection for experiments (a) cld.1 and (b) cld.2. Open circles, high; solid circles, low.

atmosphere (cloud water, rainwater, pristine ice crystals, snow, aggregates, graupel and hail). This complexity level includes the precipitation process. Frozen and mixed phased hydrometeors were not included in the analysis because the simulations did not produce any significant amount of these categories.

[24] A single grid was used (104 × 99 grid points) covering a small portion of the northern coast of the island of Puerto Rico, centered at the AO, with a horizontal resolution of 1km (Figure 1, expanded inset). For the vertical coordinate a grid spacing of 100 m was used near the surface and was stretched at a constant ratio of 1.1 until ΔZ reached 1000 m. The model depth is 22.83 km with 40 vertical layers.

5.2. Results

[25] In this section the results from the different idealized experiments are presented, with special emphasis on the cloud water content (CW), rainwater content (RW), and total liquid water (LW) vertical profiles. The profiles are plotted at the time and location of maximum hydrometeor production of each set of experiments. Figure 10 shows the vertical profiles of CW, RW, and LW for the three simulations of both cld.1 and cld.2.

[26] The cloud water mixing ratio field follows the same pattern in the two experiments. In Figure 10 it is clearly seen that cloud droplet production is significantly larger at low levels (below 1500 m), and at higher levels (between 3 and 4 km) in polluted air than in unpolluted skies, represented by the high and low runs, respectively. However, the rainwater mixing ratio in polluted air is less than a third of that in unpolluted air for the cld.1 runs, and almost nonexistent in the cld.2 experiment. *Khain et al.* [1999] argue that this is attributed to the possible fact that drop concentration in runs similar to high is several times larger than in low, and therefore cloud droplets in high are significantly smaller than in low. A look at the vertical profiles of cloud droplet number concentration for the cases of polluted and pristine maritime air in experiments cld.1 and cld.2 shows this trend, as depicted in Figure 11. At some heights between the lowest levels and 2500 km, the droplet concentration in polluted air was the double than that in unpolluted air for the first set of experiments.

[27] Another possible explanation is, given that droplet production is enhanced in polluted air, the competition for vapor growth will increase resulting in a higher concentration of smaller droplets. Consequently, these droplets do not reach the necessary radius to fall within the cloud, and therefore grow by processes of collision and coalescence. This statement agrees with observational studies of smoky and unpolluted cumulus clouds in the Amazon and Southeast Asia, as indicated earlier in this document.

[28] It is also seen that there is a burst of rainwater production at high levels, between 2.5 and 4 km, in the polluted air experiments, especially in the cld.2 plots. The cld.2 runs present no significant amount of cloud water at

altitudes above 2 km (Figure 10). These results agree with recent work reported in the compilation made by *Khain et al.* [2000]. Thus cloud-aerosol interaction impacts crucially the cloud microphysics via the influence on the droplet spectrum width.

6. Summary and Conclusions

[29] A new microphysics module incorporated to the Regional Atmospheric Modeling System, and atmospheric particle observations performed at the Arecibo Observatory were used to simulate two short precipitation events, and to investigate the possible effects of AP on cloud formation and rain development. The detailed AP observations are time varying and domain homogeneous. The first experiment showed the model's ability to simulate actual precipitation events recorded over the Observatory area using the recent AP data set, obtained with portable radiometers and spanning an entire year. This experiment also included a model run with the same configuration but a different AP and cloud spectrum; these results produced 15% less precipitation than the run combining CCN/GCCN activation and new AP concentrations. The second set of idealized runs showed that the cloud water mixing ratio and cloud droplet production is significantly larger in polluted air than in unpolluted skies and that rainwater in polluted air is less than that in unpolluted air (Figures 10 and 11). This might be due to the possible fact that if a given droplet production is enhanced in polluted air, competition for growth by vapor diffusion among existing droplets will increase, consequently, they will not reach the necessary radius to fall within the cloud, and therefore grow by processes of collision and coalescence. This in turn could explain the fact that run 1 predicted more precipitation than run 2 and run 3 in the actual precipitation event.

[30] The next step in our attempt to produce more accurate and more realistic precipitation predictions using a cloud-resolving mesoscale model is to ingest vertical profiles of atmospheric particle concentrations. Improvements could be made in the methodology of assimilating the AP information into the atmospheric model.

[31] **Acknowledgments.** This research is being conducted with the support of the NASA-EPSCOR program of the University of Puerto Rico. The atmospheric model simulations were performed at the High Performance Computing Facilities in Rio Piedras. The Arecibo Observatory is operated by Cornell University under a cooperative agreement with the National Science Foundation. Thanks are owed to Steve Saleeby at Colorado State University for providing the new cloud microphysics module for the atmospheric model, and instructions on its use.

References

Berry, E. X., and R. L. Reinhardt (1974), An analysis of cloud drop growth by collection: Part I Double distributions, *J. Atmos. Sci.*, *31*, 1814–1824.

Comarazamy, D. E. (2001), Atmospheric modeling of the Caribbean region: Precipitation and wind analysis in Puerto Rico for April 1998, M.S. thesis, 95 pp., Dep. of Mech. Eng., Univ. of P.R., Mayagüez.

Cotton, W. R., et al. (2003), RAMS 2001: Current status and future directions, *Meteorol. Atmos. Phys.*, *82*, 5–29.

Daly, C., E. H. Helmer, and M. Quiñones (2003), Mapping the climate of Puerto Rico, Vieques and Culebra, *Int. J. Climatol.*, *23*, 1359–1381.

Dubovik, O., and M. D. King (2000), A flexible inversion algorithm for retrieval of aerosol optical properties from Sun and sky radiance measurements, *J. Geophys. Res.*, *105*, 20,673–20,696.

Grabowski, W. W. (2000), Cloud microphysics and the tropical climate: Cloud-resolving model perspective, *J. Clim.*, *13*, 2306–2322.

Grabowski, W. W. (2003), Impact of cloud microphysics on convective-radiative quasi equilibrium revealed by cloud-resolving convection parameterization, *J. Clim.*, *16*, 3463–3475.

Grabowski, W. W., X. Wu, and M. T. Moncrieff (1999), Cloud resolving modeling of tropical cloud systems during Phase III of GATE. Part III: Effects of cloud microphysics, *J. Atmos. Sci.*, *56*, 2384–2402.

Ichoku, C., et al. (2002), Analysis of the performance characteristics of the five-channel Microtops II Sun photometer for measuring aerosol optical thickness and precipitable water vapor, *J. Geophys. Res.*, *107*(D13), 4179, doi:10.1029/2001JD001302.

Jonas, P. R. (1996), Turbulence and cloud microphysics, *Atmos. Res.*, *40*, 283–306.

Kaufman, Y. J., and T. Nakajima (1993), Effect of Amazon smoke on cloud microphysics and albedo-analysis from satellite imagery, *J. Appl. Meteorol.*, *32*, 729–744.

Khain, A. P., A. Pokrovsky, and I. Sednev (1999), Some effects of cloud-aerosol interaction on cloud microphysics structure and precipitation formation: Numerical experiments with a spectral microphysics cloud ensemble model, *Atmos. Res.*, *52*, 195–220.

Khain, A., M. Ovtchinnikov, M. Pinsky, A. Pokrovsky, and H. Krugliak (2000), Notes on the state-of-the-art numerical modeling of cloud microphysics, *Atmos. Res.*, *55*, 159–224.

King, M. D., D. M. Byrne, B. M. Herman, and J. A. Reagan (1978), Aerosol size distributions obtained by inversion of spectral optical depth measurements, *J. Atmos. Sci.*, *35*, 2153–2167.

Li, X., C. H. Sui, and K. M. Lau (2002), Dominant cloud microphysics processes in a tropical oceanic convective system: A 2D cloud resolving modeling study, *Mon. Weather Rev.*, *130*, 2481–2491.

Liu, Y., D. L. Zhang, and M. K. Yau (1997), A multiscale numerical study of Hurricane Andrews, 1992. Part I: Explicit simulation and verification, *Mon. Weather Rev.*, *125*, 1065–1092.

Malmgren, B. A., and A. Winter (1999), Climate zonation in Puerto Rico based on principal components analysis and an artificial neural network, *J. Clim.*, *12*(4), 977–985.

Meyers, M. P., R. L. Walko, J. Y. Harrington, and W. R. Cotton (1997), New RAMS cloud microphysics parameterization. Part II: The two-moment scheme, *Atmos. Res.*, *45*, 3–39.

Nagel, D., A. Herber, L. W. Thomason, and U. Leiterer (1998), Vertical distribution of the spectral aerosol optical depth in the Arctic from 1993 to 1996, *J. Geophys. Res.*, *103*(D2), 1857–1870.

Pielke, R. A., et al. (1992), A comprehensive meteorological modeling system-RAMS, *Meteorol. Atmos. Phys.*, *49*, 69–91.

Rogers, R. R., and M. K. Yau (1996), *A Short Course in Cloud Physics*, 290 pp., Elsevier, New York.

Saleeby, M. S., and W. R. Cotton (2004), A large-droplet mode and prognostic number concentration of cloud droplets in the Colorado State University Regional Atmospheric Modeling System (RAMS), Part I: Module descriptions and supercell test simulations, *J. Appl. Meteorol.*, *43*, 182–195.

Taylor, M. A., D. B. Enfield, and A. A. Chen (2002), Influence of the tropical Atlantic versus the tropical Pacific on Caribbean rainfall, *J. Geophys. Res.*, *107*(C9), 3127, doi:10.1029/2001JC001097.

Walko, R. L., C. J. Tremback, and F. A. Herstenstein (1995a), The Regional Atmospheric Modeling System technical description, report, Atmos., Meteorol., and Environ. Technol., Boulder, Colo.

Walko, R. L., C. J. Tremback, and F. A. Herstenstein (1995b), The Regional Atmospheric Modeling System user's guide, input parameters and variables, report, Atmos., Meteorol., and Environ. Technol., Boulder, Colo.

Walko, R. L., W. R. Cotton, M. P. Meyers, and J. Y. Harrington (1995c), New RAMS cloud microphysics parameterization: Part I: The single-moment scheme, *Atmos. Res.*, *38*, 29–62.

Wang, Y. (2002), An explicit simulation of tropical cyclones with a triply nested movable mesh primitive equation model: TCM3. Part II: Model refinements and sensitivity to cloud microphysics parameterization, *Mon. Weather Rev.*, *130*, 3022–3036.

D. E. Comarazamy and R. V. R. Pandya, Mechanical Engineering Department, University of Puerto Rico, Mayagüez, PR 00681-9000. (comarazamy@me.uprm.edu)

J. E. Gonzalez, Mechanical Engineering Department, Santa Clara University, Santa Clara, CA 95053, USA.

S. Raizada and C. A. Tepley, National Astronomy and Ionosphere Center, Arecibo Observatory, Arecibo, PR 00612.